LARGE-SCALE REGULAR MORPHOLOGICAL PATTERNS IN THE RADIO JET OF NGC 6251

Hiroshi Sudou & Yoshiaki Taniguchi

Astronomical Institute, Graduate School of Science, Tohoku University, Aoba, Sendai 980-8578, Japan

Received _____; accepted _____

ABSTRACT

We report on large-scale, regular morphological patterns found in the radio jet of the nearby radio galaxy NGC 6251. Investigating morphological properties of this radio jet from the nucleus to a radial distance of ~ 300 arcsec (≈ 140 kpc) mapped at 1662 MHz and 4885 MHz by Perley, Bridle, & Willis, we find three chains, each of which consists of five radio knots. We also find that eight radio knots in the first two chains consist of three small sub-knots (the triple-knotty substructures). We discuss the observational properties of these regular morphological patterns.

Subject headings: galaxies – individual (NGC 6251): galaxies - jets: galaxies: active – radio continuum: galaxies

1. INTRODUCTION

Since the discovery of the powerful radio jet from quasar 3C273 (Hazard et al. 1963, see for a review Bridle & Perley 1984; Zensus 1997), the generation of radio jets has been one of the long-standing main problems in active galactic nuclei (e.g., Begelman, Blandford, & Rees 1984; Urry & Padovani 1995). The most probable energy sources have been considered to be either mass-accreting, supermassive, single black holes around which gravitational energy is transformed into huge kinetic and radiation energies with the help of gaseous accretion disks (e.g., Rees 1984) or the electromagnetic extraction of energy from spinning supermassive black holes (Blandford & Znajek 1977; see also Wilson & Colbert 1995). In order to understand the genesis of radio jets, it is important to find some reliable observational constraints on theoretical models.

It has been noticed that parsec-scale radio jets probed by VLBI techniques often show wiggles (e.g., Whitmore & Matese 1981; Roos 1988; Roos, Kaastra, & Hummel 1993). If a certain mechanism responsible for the formation of the wiggles (e.g., the precession of a supermassive black hole binary; Begelman, Blandford, & Rees 1980) has been working since the onset of radio jet activity, there could be some morphological evidence even in well-developed (i.e., $\sim$ 100 kpc scale) radio jets. Furthermore, recent progress in three-dimensional numerical MHD simulations has enabled us to examine the detail of morphological properties of radio jets due to the so-called Kelvin-Holmheltz instability in the magnetic fluid (e.g., Rosen et al. 1998; Koide, Shibata, & Kudoh 1999). Therefore, since morphological properties of actual radio jets provide important constraints on the physical process involved in radio jets, it is interesting to investigate overall morphological properties of some well-developed radio jets in detail.

For this purpose, in this paper, we investigate morphological properties of the radio jet of NGC 6251 in detail because the radio jet of NGC 6251 is one of the brightest known

examples of a well-developed jet (Waggett, Warner, & Baldwin 1977; Cohen & Readhead 1979; Perley, Bridle, & Willis 1984; Jones et al. 1986; Jones & Wehrle 1994). We use a distance to NGC 6251, 94.4 Mpc, which is determined with the use of a recession velocity of NGC 6251 to the galactic standard of rest, $V_{\rm GSR} = 7079$ km s^{-1} (de Vaucouleurs et al. 1991), and a Hubble constant, $H_0 = 75$ km s^{-1} Mpc^{-1}.

2. RESULTS

2.1. A Large-scale Regular Morphological Pattern

First, we investigate large-scale morphological properties of the radio jet of NGC 6251 using the radio continuum image at 4885 MHz obtained by Perley et al. (1984; see the right panel of Figure 5 in their paper). In the top panel of Figure 1, we show the image from the radio nucleus to a radius of ~ 300 arcsec (≈ 140 kpc). The spatial resolution of this image is 4.4 arcsec. There can be seen more than a dozen knots along the radio jet. We find that there are three sets of radio knots; hereafter Chain A, B, and C (see Figure 1). Each chain appears to consist of five knots although the first knot in Chain A can be marginally discerned because it is so close to the radio nucleus. The fifth knot in each Chain is slightly displaced outward with respect to the inner four knots.

In order to examine whether or not these Chains show some regular patterns, we measure the positions of 15 knots; the measurements are made using a scale on an enlarged photocopy of the image shown in Figure 1. The measurement error is ≈ 0.5 mm on the photocopy, corresponding to ≈ 0.6 arcsec; note that the actual measurement error is about 0.1 mm on the photocopy but the ambiguity of the peak of radio knots is estimated to be ≈ 0.5 mm. The following quantities are measured in our analysis (see Figure 2). 1) d and D: the radial distance in units of arcsec and kpc respectively, 2) s and S: the

separation between adjacent knots in units of arcsec and kpc respectively, and 3) w and W: the separation of the i-th knot between the adjacent Chains in units of arcsec and kpc respectively. The results are summarized in Table 1.

In Figure 3, we show the angular distances (d) of the fifteen knots found in three Chains A, B, and C. It is shown that the knots do not develop linearly in distance; the five knots in Chain C are more distant than the position extrapolated using the positions of the five knots in both Chains A and B. In order to see this property quantitatively, we show the separations of the i-th knot between two different Chains (w) in Figure 4. The separations between Chains B and C [w(B-C)] are systematically larger than those between Chains A and B [w(A-B)]; i.e., w(A-B) $\simeq$ 67 – 89 arcsec while w(B-C) $\simeq$ 120 – 132 arcsec, corresponding to linear separations of W(A-B) $\simeq$ 42 – 55 kpc and W(B-C) $\simeq$ 75 – 82 kpc.

In Figure 5, we show the angular separation between two adjacent knots. The separation appears to be increasing with increasing distance although there can be seen some scatters in the data points.

Another interesting property found in Figure 1 is that the separations among the five knots appear to be larger for the outer Chain. In Figure 6, we show the separations between two adjacent knots (s) in three Chains separately. The separations increase from Chain A through B to C. It is also found that the variation patterns in $s[(i+1)$ - $i]$ from $i = 1$ to 4 are quite similar among three Chains. These findings reinforce that our identifications of three Chains are really meaningful. It is thus suggested that the radio jet activity in NGC 6251 is not sporadic but regular with some periodicity.

2.2. Substructures in Radio Knots

We further investigate detailed morphological properties of the individual radio knots. To perform this, we use the radio continuum image at 1662 MHz given by Perley et al. (1984; see Figure 4 in their paper). This map covers the inner 2 arcmin ($\approx$ 55 kpc) region of the radio jet with the spatial resolution of 1.15 arcsec. In Figure 7, we show the map together with close-up images of eight individual knots; the first four knots are in Chain A (A2, A3, A4, and A5) and the remaining four knots are in Chain B (B1, B2, B3, and B4). These identifications are the same as those in section 2.1 (see Table 1). Each knot appears to consist of three brightness peaks; hereafter the triple-knotty substructure. In particular, this substructure is unambiguously seen in the first two knots, A2 and A3.

3. DISCUSSION

We have shown that there are two kinds of regular morphological structures in the radio jet of NGC 6251; 1) three Chains consisting of five radio knots , and 2) the triple-knotty substructures in the individual knots. Here we discuss some possible origins of these large-scale regular structures.

3.1. Chains

The presence of three Chains suggests that a certain periodicity is involved in the radio jet activity of NGC 6251. As shown in Table 1, the separations of the i-th knots (W) are quite similar between two adjacent Chains; i.e., the average values are $\overline{W}$(A-B) $\simeq 48.0 \pm 0.5$ kpc and $\overline{W}$(B-C) $\simeq 79.3 \pm 2.9$ kpc. We estimate timescales corresponding to these separations. In order to perform this, both the viewing angle toward the jet ($\theta_{\rm jet}$) and the jet velocity ($v_{\rm jet}$) are necessary for the kpc-scale radio jet.

Since the parsec-scale counterjet cannot be seen in the previous VLBI observations (Perley et al. 1984; Jones et al. 1986; Jones & Wehrle 1994; see however Sudou et al. 2000a, b), it is unlikely that the radio jet of NGC 6251 lies close to the celestial plane. Jones et al. (1986) estimate that the angle between the radio jet and our line of sight may be $\theta_{\rm jet} \sim 45^\circ$ based on the observed jet-to-counterjet intensity ratio. We therefore adopt $\theta_{\rm jet} = 45^\circ$ in later analysis. Another important quantity is the large-scale (i.e., kpc-scale) jet velocity $v_{\rm jet}$ which is also difficult to be estimated (e.g., Perley et al. 1984). Based on several constraints (e.g., the energy flux required to power the radio jet, etc.), Perley et al. (1984) suggest that the large-scale jet velocity of NGC 6251 is subrelativistic; $v_{\rm jet} \leq 0.1c$. It is known that ram pressure confinement for the strongest double-lobed radio sources such as NGC 6251 requires $v_{\rm jet} \simeq 0.1c$ (e.g., Begelman et al. 1984). On the other hand, using the observed jet-to-counterjet brightness ratio, Jones et al. (1986) suggests $v_{\rm jet} \cos\theta_{\rm jet} \geq 0.6$ for brightness ratio ≥ 30. Given $\theta_{\rm jet} = 45^\circ$, they obtain $v_{\rm jet} \sim 0.84c$. Since this estimate seems more reliable, we adopt for simplicity $v_{\rm jet} = 0.8c$ in later analysis. These assumptions (i.e., $\theta_{\rm jet} = 45^\circ$ and $v_{\rm jet} = 0.8c$) seem enough to estimate rough timescales related to the large-scale regular structures found in this study.

First we estimate timescales related to three Chains A, B, and C. Since the jet velocity is relativistic, we have to take account of the relativistic aberration effect. The true projected distance of the radio jet from the nucleus is estimated as $D'_{\rm jet} = \delta\ D_{\rm jet}$ where δ is the Doppler factor defined as $\delta = [\gamma(1 - (v_{\rm jet}/c)\cos\theta_{\rm jet})]^{-1}$ where $\gamma = [1 - (v_{\rm jet}/c)^2]^{-1/2}$. Thus the true length of the radio jet is estimated as $L^0_{\rm jet} = D'_{\rm jet}(\sin\theta_{\rm jet})^{-1}$. Therefore, the related timescale $\tau_{\rm jet}$ is estimated as

$$\begin{aligned} \tau_{\rm jet} &= L^0_{\rm jet}/v_{\rm jet} \\ &= D'_{\rm jet}/(0.8c\ \sin\theta_{\rm jet}) \end{aligned}$$

$$\simeq 1.83 \times 10^{11}\ \delta\ D_{\rm jet,1}\ v_{\rm jet,0.8}^{-1}\ (\sin\theta_{\rm jet,45})^{-1}\ {\rm s}$$
$$\simeq 5.79 \times 10^{3}\ \delta\ D_{\rm jet,1}\ v_{\rm jet,0.8}^{-1}\ (\sin\theta_{\rm jet,45})^{-1}\ {\rm y} \quad (1)$$

where $D_{\rm jet,1}$ is the jet length projected onto the celestial plane in units of 1 kpc, $v_{\rm jet,0.8}$ is the jet velocity in units of $0.8c$, and $\theta_{\rm jet,45}$ is the jet viewing angle in units of 45°. Given the velocity and viewing angle assumed above, we obtain $\delta = 1.38$. The projected jet lengths of three Chains are $D_{\rm jet}({\rm A}) = D_5({\rm A}) - D_1({\rm A}) = 32.4 - 3.6 = 28.8$ kpc, $D_{\rm jet}({\rm B}) = D_5({\rm B}) - D_1({\rm B}) = 87.8 - 45.5 = 42.3$ kpc, and $D_{\rm jet}({\rm C}) = D_5({\rm C}) - D_1({\rm C}) = 169.9 - 120.7 = 49.2$ kpc. Then we obtain the durations required to develop the radio jet for three Chains; $\tau_{\rm jet}({\rm A}) \approx 2.3 \times 10^5$ years, $\tau_{\rm jet}({\rm B}) \approx 3.4 \times 10^5$ years, and $\tau_{\rm jet}({\rm C}) \approx 3.9 \times 10^5$ years. These durations are shorten by one order of magnitude than the precession period estimated by Jones et al. (1986; see also Begelman et al. 1980), $\tau_{\rm prec} \simeq 1.8 \times 10^6$ y. This precession is proposed to explain the global wiggle pattern of the radio jet of NGC 6251.

As estimated above, the length of Chain becomes longer with increasing radial distance; i.e., $D_{\rm jet}({\rm A}) < D_{\rm jet}({\rm B}) < D_{\rm jet}({\rm C})$. If this tendency is real, the radio jet of NGC 6251 must be accelerated even at several tens of kpc. An alternative idea may be that the radio jet is bending in a plane which encloses the radio jet and our line of sight to the jet. Since the position angle of the parsec-scale radio jet (PA = 302°.2 ± 0°.8, for the epoch of 1950.0; Cohen & Readhead 1979) is slightly different from that of the kpc-scale jet (PA = 296°.5; Waggett et al. 1977), Cohen & Readhead (1979) suggest a possible bending of the radio jet of NGC 6251. Therefore, it is interesting to investigate this idea in more detail.

Here we assume that the true jet lengths of three Chains are nearly the same and the observed differences among them are attributed to the differences in the viewing angle toward them. If this is the case, we obtain the following relation;

$$\frac{D_{\rm jet}({\rm A})\ \delta({\rm A})}{\sin\theta_{\rm jet}({\rm A})} = \frac{D_{\rm jet}({\rm B})\ \delta({\rm B})}{\sin\theta_{\rm jet}({\rm B})} = \frac{D_{\rm jet}({\rm C})\ \delta({\rm C})}{\sin\theta_{\rm jet}({\rm C})} \tag{2}$$

where $\theta_{\rm jet}$(A), $\theta_{\rm jet}$(B), and $\theta_{\rm jet}$(C) are the average viewing angles toward Chain A, B, and C, and δ(A), δ(B), and δ(C) are the average Doppler factors toward Chain A, B, and C, respectively. If we adopt $\theta_{\rm jet}({\rm C}) = 45.0^\circ$ and $\delta({\rm C}) = 1.38$, we obtain $\theta_{\rm jet}({\rm A}) \simeq 33.1^\circ$ and $\theta_{\rm jet}({\rm B}) \simeq 41.3^\circ$, with $\delta({\rm A}) \simeq 1.82$ and $\delta({\rm B}) \simeq 1.50$. It is therefore suggested that the direction of the radio jet is approaching the line of sight as time goes by, or the jet flow follows fixed but bent path. This result is schematically illustrated in Figure 8.

Recently, Sudou et al. (2000a, b) have found the counterjet at sub-parsec scale and estimated the viewing angle to the sub-pc scale jet $\theta_{\rm jet} \simeq 17^\circ - 31^\circ$. Since the viewing angle toward Chain A derived above is consistent with their new estimate, this bending jet model appears consistent with the observation. Therefore, it is not necessary to introduce the jet acceleration at kpc regions.

3.2. The Knots in Chains

We investigate the separations of the knots in three Chains. An average separation of the knots in each Chain is; $\overline{S} = \sum_{i=1}^{4} S_{[i+1]-1}/4 \simeq 7.2 \pm 2.9$ kpc for Chain A, 10.6 ± 4.5 kpc for Chain B, and 12.3 ± 3.1 kpc for Chain C. Therefore, the average separation appears to increase with increasing Chain number. It is noted that the fifth knot in each Chain is located at a larger distance than that expected from the separations for the remaining four knots (see column 5 of Table 1). If we omit the data of the fifth knot, we obtain average separations of $\overline{S} = \sum_{i=1}^{3} S_{[i+1]-1}/3 \simeq 5.6 \pm 1.0$ kpc for Chain A, 8.1 ± 1.6 kpc for Chain B, and 10.6 ± 1.2 kpc for Chain C. Although the tendency holds, the average separations are smaller than the former estimates respectively. If we adopt the bending jet model described in section 3.2 together with the relativistic aberration

effect, the true separation, $S^0 = \delta\overline{S}/\sin\theta_{\rm jet}$, is; $S^0({\rm A}) \simeq 5.6 \times 1.82/\sin 33.1^\circ \simeq 18.7$ kpc, $S^0({\rm B}) \simeq 8.1 \times 1.50/\sin 41.3^\circ \simeq 18.4$ kpc, and $S^0({\rm C}) \simeq 10.6 \times 1.38/\sin 45^\circ \simeq 20.7$ kpc. These values are similar to each other.

We obtain an average separation of the knots in three Chains of $\simeq 19.2$ kpc, corresponding to a timescale of $\simeq 7.8 \times 10^4$ years given the jet velocity of $v_{\rm jet} = 0.8c$.

3.3. The Triple-Knotty Substructure

We discuss briefly observational properties of the triple-knotty substructures. As shown in Figure 7, the first two knots (A2 and A3) show a clear triple-knotty substructures. However, the others show a range of irregular, complex morphologies although we give possible identifications of the triple knots for them by arrows. It is interesting to mention that such a triple-knotty substructure is also found in the radio jet of Centaurus A (Clarke et al. 1986).

3.4. Concluding Remarks

In summary, the large-scale, regular morphological patterns involve the three kinds of structures; Chains, knots, and triple-knotty substructures in the knots. The concerned timescales for the first two structures are $\sim 10^5$ years and $\sim 10^4$ years, respectively. Although the longest timescale obtained for Chains may be related to the precession motion, the other two timescales are not understood easily.

Although some studies of the large-scale morphological properties of the radio jets have been carried out (e.g., Perley & Bridle 1984, Sparks et al. 1996, Perlman et al. 1999, Biretta et al. 1999, Bahcall et al. 1995, Röser et al. 1996, and Clarke et al. 1986), the

analysis presented in this paper is the first trial to investigate large-scale morphological regularity of radio jets. Since this kind of analysis needs high-resolution and large-scale radio continuum mapping, it seems difficult to perform a systematic morphological study of radio jets. Therefore, at present, it is difficult to judge whether or not large-scale morphological patterns found in the radio jet of NGC 6251 are general properties. However, this kind of analysis will be important to provide observational constraints on the theory for radio jets.

We thank to Dr. D. Jones and anonymous referee for their useful comments and suggestions. This work was financially supported in part by Grant-in-Aids for the Scientific Research (Nos. 10044052, and 10304013) of the Japanese Ministry of Education, Culture, Sports, and Science.

REFERENCES

Bahcall, J. N., Kirhakos, S., Schneider, D. P., Davis, R. J., Muxlow, T. W. B., Garrington, S. T., Conway, R. G., & Unwin, S. C. 1995, ApJ, 452, L91

Begelman, M. C., Blandford, R. D., & Rees, M. J. 1980, Nature, 287, 307

Begelman, M. C., Blandford, R. D., & Rees, M. J. 1984, Rev. Modern Phys. 56, 255

Biretta, J. A., Sparks, W. B., & Macchetto, F. 1999, ApJ, 520, 621

Blandford, R. D., & Znajek, R. L. 1977, MNRAS, 179, 433

Bridle, A. H., & Perley, R. A. 1984, ARA&A, 22, 319

Clarke, D. A., Burns, J. O., & Feigelson, E. D. 1986, ApJ, 300, L41

Cohen, M. H., & Readhead, A. C. S. 1979, ApJ, 233, L101

de Vaucouleurs, G., de Vaucouleurs, A., Corwin, C. Jr., Buta, R. J. Paturel, G., & Fouqúe, P. 1991, Third Reference Catalogue of Bright Galaxies. (Springer-Verlag)

Hazard, C., Mackey, M. B., & Shimmins, A. J. 1963, Nature, 197, 1037

Jones, D. L., et al. 1986, ApJ, 305, 684

Jones, D. L., & Wehrle, A. E. 1994, ApJ, 427, 221

Koide, S., Shibata, K., & Kudoh, T. 1999, ApJ, 522, 727

Perley, R. A., Bridle, A. H., & Willis, A. G. 1984, ApJS, 54, 291

Perlman, E. S., Biretta, J. A., Sparks W. B., & Macchetto, F. 1999, ApJ, 117, 2185

Rees, M. J. 1984, ARA & A, 22, 471

Roos, N. 1988, ApJ, 334, 9

Roos, N., Kaastra, J. S., & Hummel, C. A. 1993, ApJ, 409, 130

Rosen, A., Hardee, P. P., Clarke, D. A., & Johnson, A. 1998, ApJ, 510, 136

Röser, H. -J., Conway, R. G., & Meisenheimer, K. 1996, A & A, 1996, 414

Sparks, W. B., Biretta, J. A., & Macchetto, F. 1996, ApJ, 473, 254

Sudou, H., Taniguchi, Y., Ohyama, Y., Kameno, S., Sawada-Satoh, S., Inoue, M., Kaburaki, O., & Sasao, T. 2000a, in Astrophysical Phenomena Revealed by Space VLBI, ed. H. Hirabayashi, P.G. Edwards, & D.W. Murphy, in press (astro-ph/0004139)

Sudou, H., Taniguchi, Y., Ohyama, Y., Kameno, S., Sawada-Satoh, S., Inoue, M., Kaburaki, O., & Sasao, T. 2000b, in preparation

Urry, C. M., & Padovani, P. 1995, PASP, 107, 803

Waggett, P. C., Warner, P. J., & Baldwin, J.E. 1977, MNRAS, 181, 465

Whitmore, D. P., & Matese, J. J. 1981, Nature, 293, 722

Wilson, A. S., & Colbert, E. J. M. 1995, ApJ, 438, 62

Zensus, J. A. 1997, ARA&A, 35, 607

Fig. 1.— The top panel shows The radio continuum image at 4885 MHz obtained by Perley et al. (1984). Three Chains A, B, and C together with the identification of radio knots are separately shown in the lower three panels.

Fig. 2.— The definitions of the quantities used in this paper (see text).

Fig. 3.— The angular distances (d) of the 15 knots are plotted against the sequential knot number.

Fig. 4.— The separations of the i-th knots between two adjacent Chains (w).

Fig. 5.— The angular separations (s) between two adjacent knots are plotted against the sequential knot number.

Fig. 6.— The angular separations among the knots in three Chains (s). are shown as a function of the knot number.

Fig. 7.— The top two panels show the radio continuum image at 1662 MHz obtained by Perley et al. (1984). The upper panel shows Chain A and the lower one shows Chain B. Close-up images of the eight radio knots are shown in the lower panel. Each arrow shows resolved substructure of the knot.

Fig. 8.— A schematic illustration of the bended jet model for the radio jet of NGC 6251.

Table 1. Basic data of the identified knots

No.	Name	d ($''$)	D (kpc)	s ($''$)	S (kpc)	w ($''$)	W (kpc)
1	A1	5.8	3.6	···	···	···	···
2	A2	13.5	8.4	7.7	4.8	···	···
3	A3	24.8	15.5	11.3	7.1	···	···
4	A4	32.8	20.5	8.0	5.0	···	···
5	A5	51.7	32.4	18.9	11.9	···	···
6	B1	72.6	45.5	···	···	66.8	41.8
7	B2	85.8	53.7	13.2	8.3	72.3	45.3
8	B3	101.6	63.6	15.8	9.9	76.8	48.1
9	B4	111.3	69.7	9.7	6.1	78.6	49.2
10	B5	140.2	87.8	28.9	18.1	88.5	55.4
11	C1	192.7	120.7	···	···	120.1	75.2
12	C2	208.8	130.8	16.2	10.1	123.1	77.1
13	C3	228.5	143.1	19.6	12.3	126.9	79.5
14	C4	243.5	152.5	15.0	9.4	132.1	82.8
15	C5	271.2	169.9	27.7	17.3	131.0	82.1

This figure "Sudou_fig1.jpg" is available in "jpg" format from:

http://arxiv.org/ps/astro-ph/0004194v1

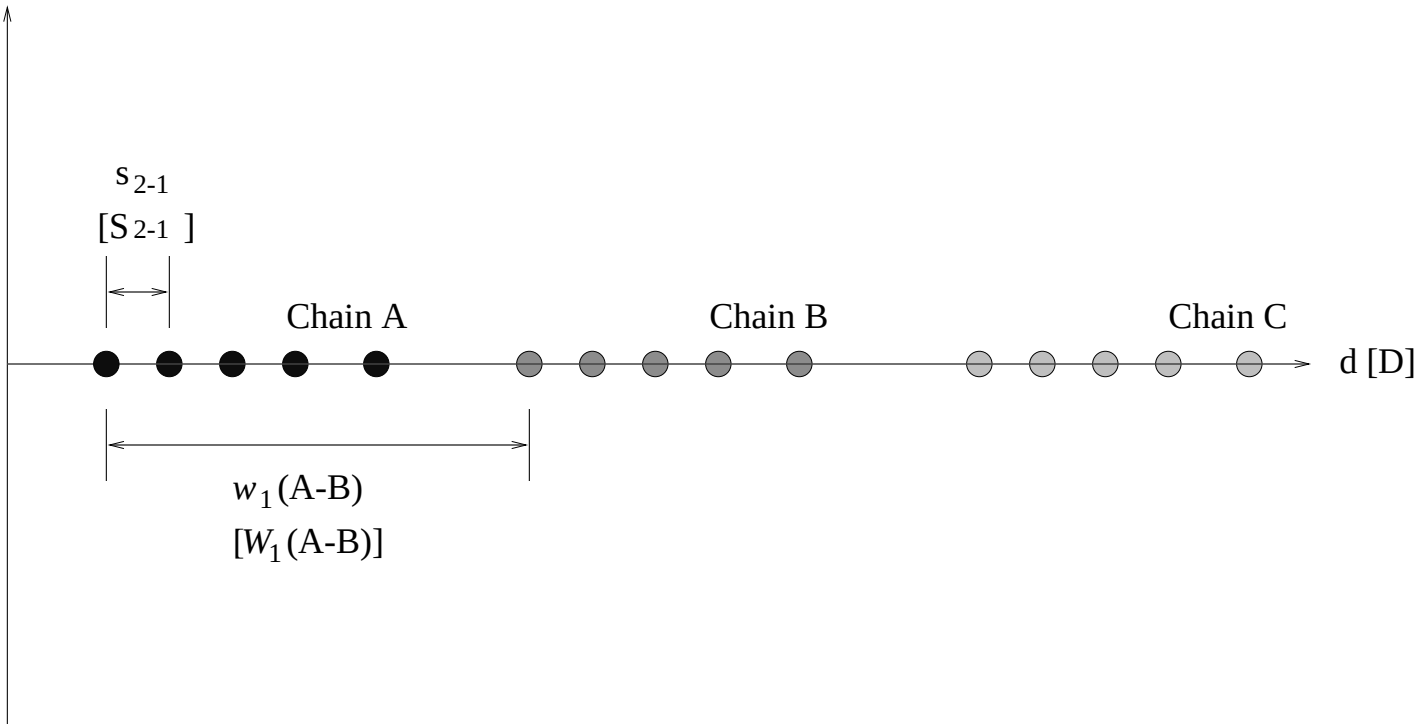
s 2-1
[S 2-1]
Chain A
Chain B
Chain C
d [D]
w_1(A-B)
[W_1(A-B)]

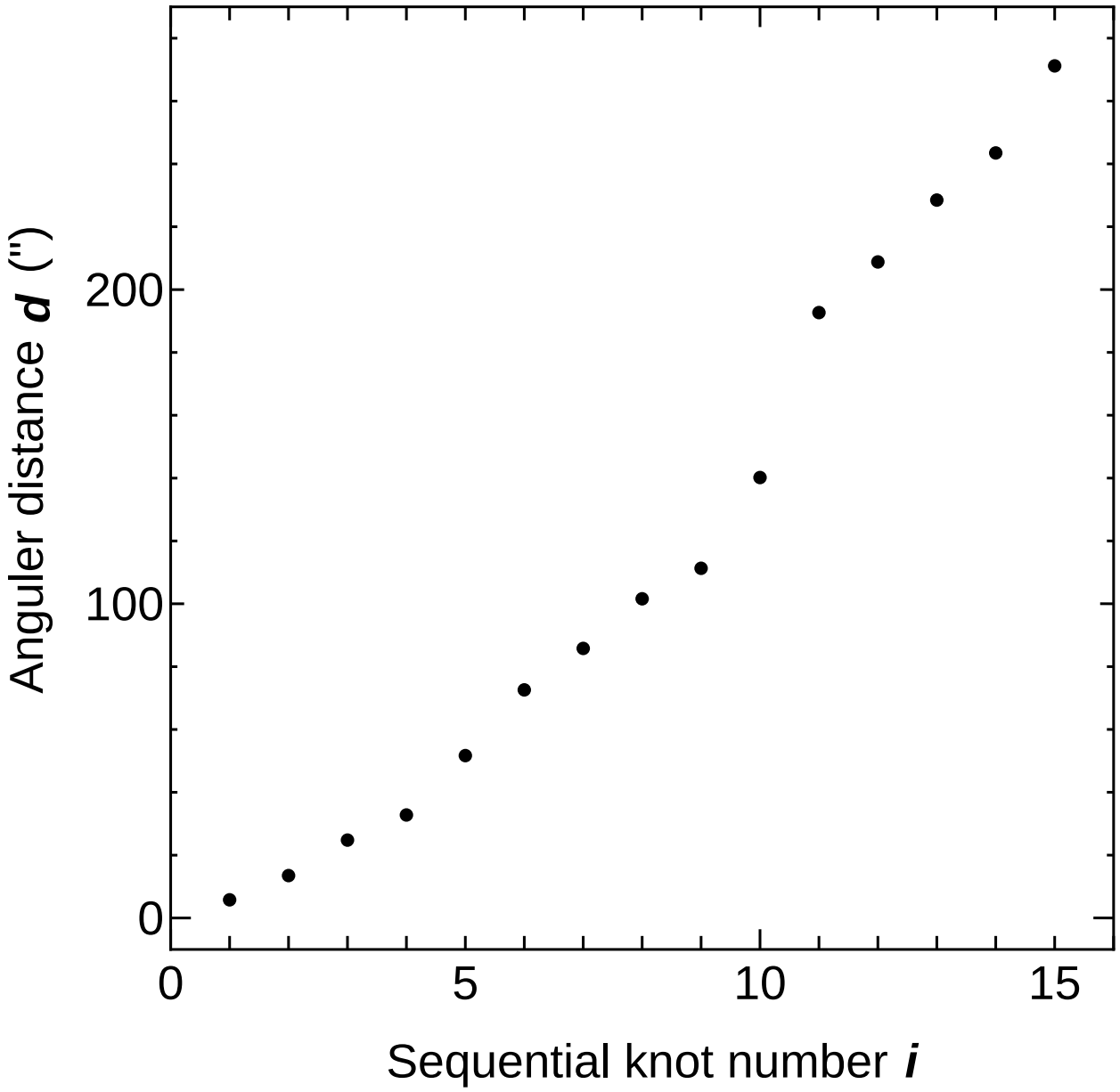
Anguler distance d (")
0
100
200
0
5
10
15
Sequential knot number i

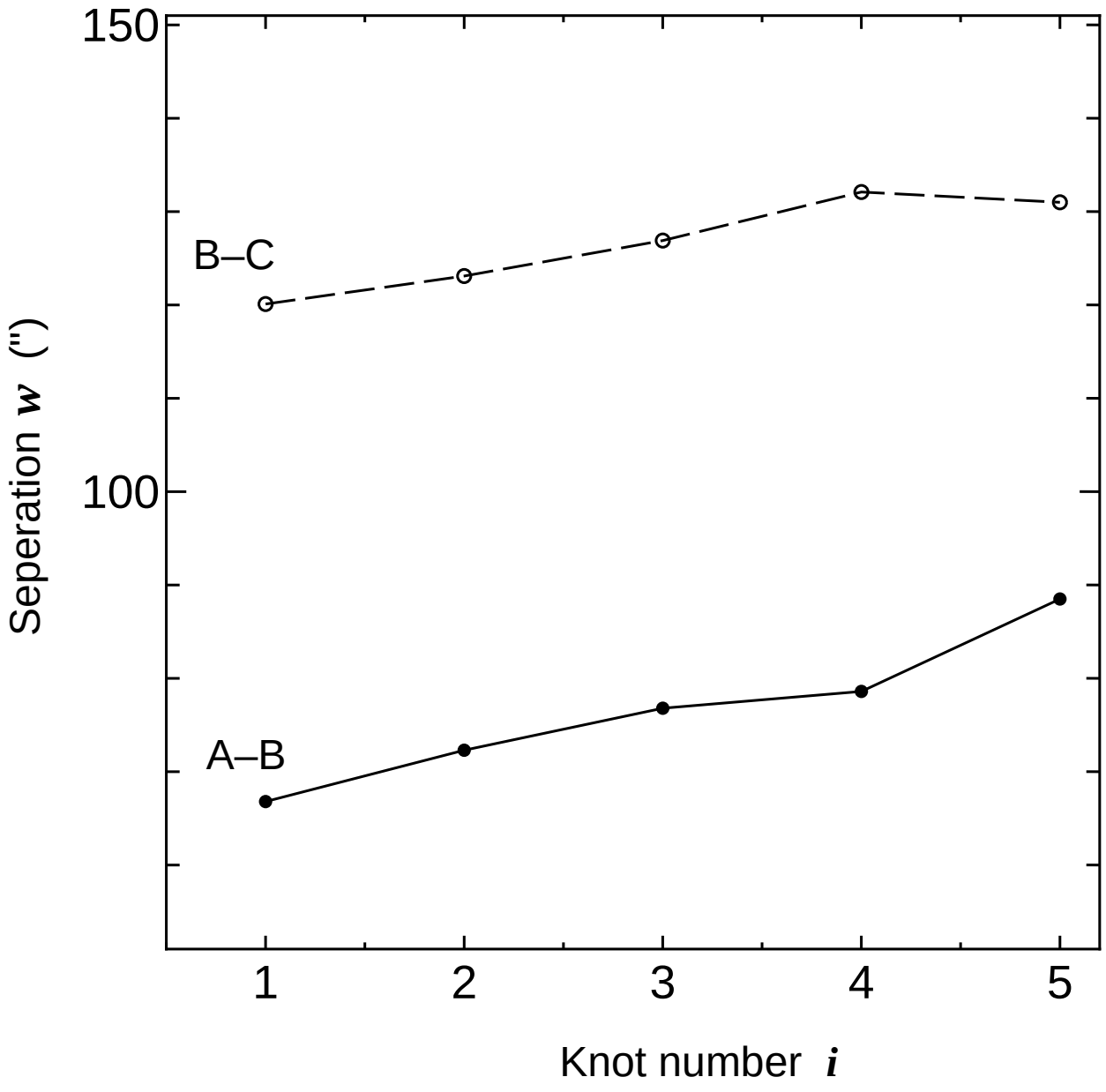
150
100
Seperation w (")
B–C
A–B
1
2
3
4
5
Knot number i

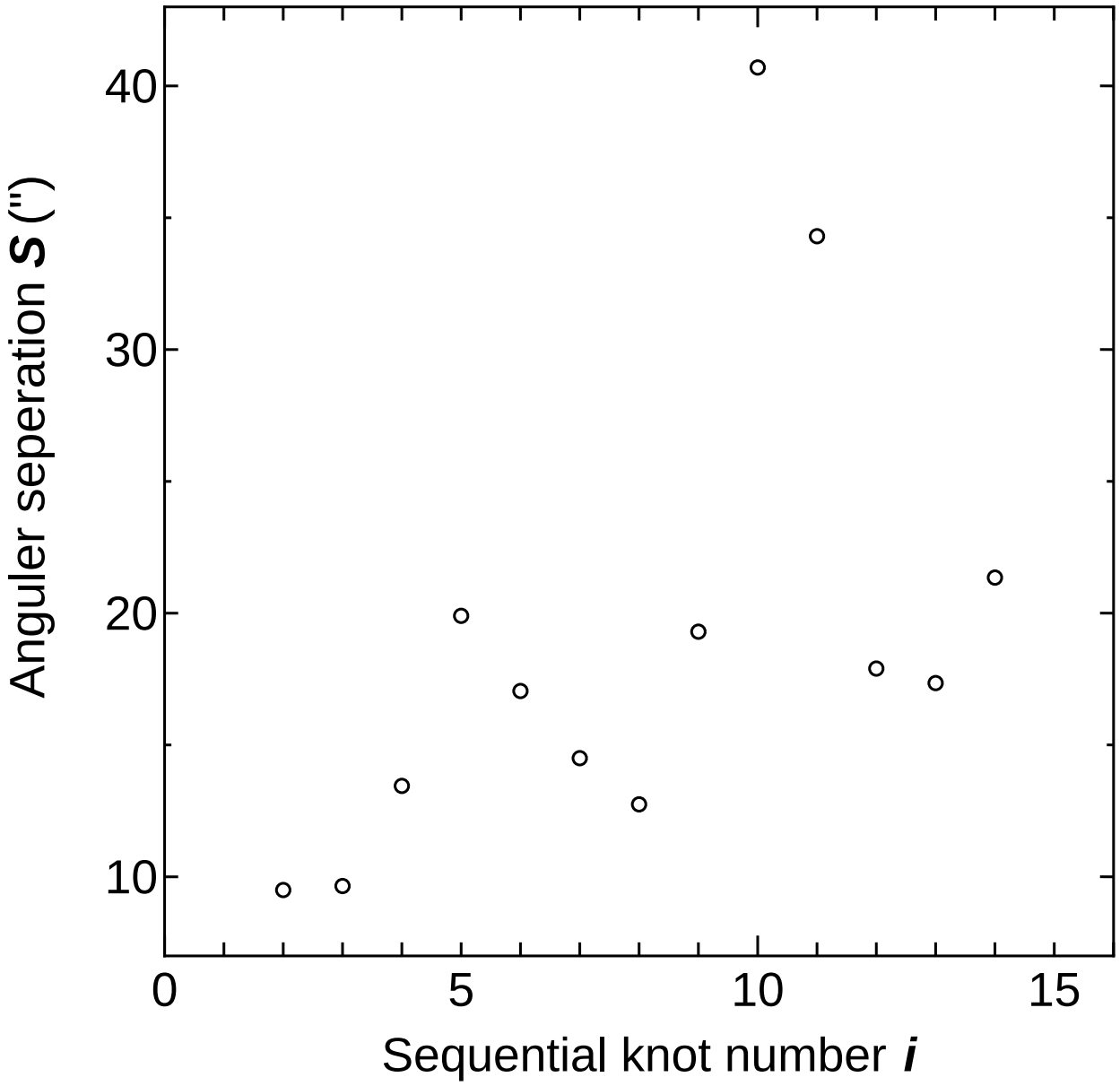
Anguler seperation S (")
40
30
20
10
0
5
10
15
Sequential knot number i

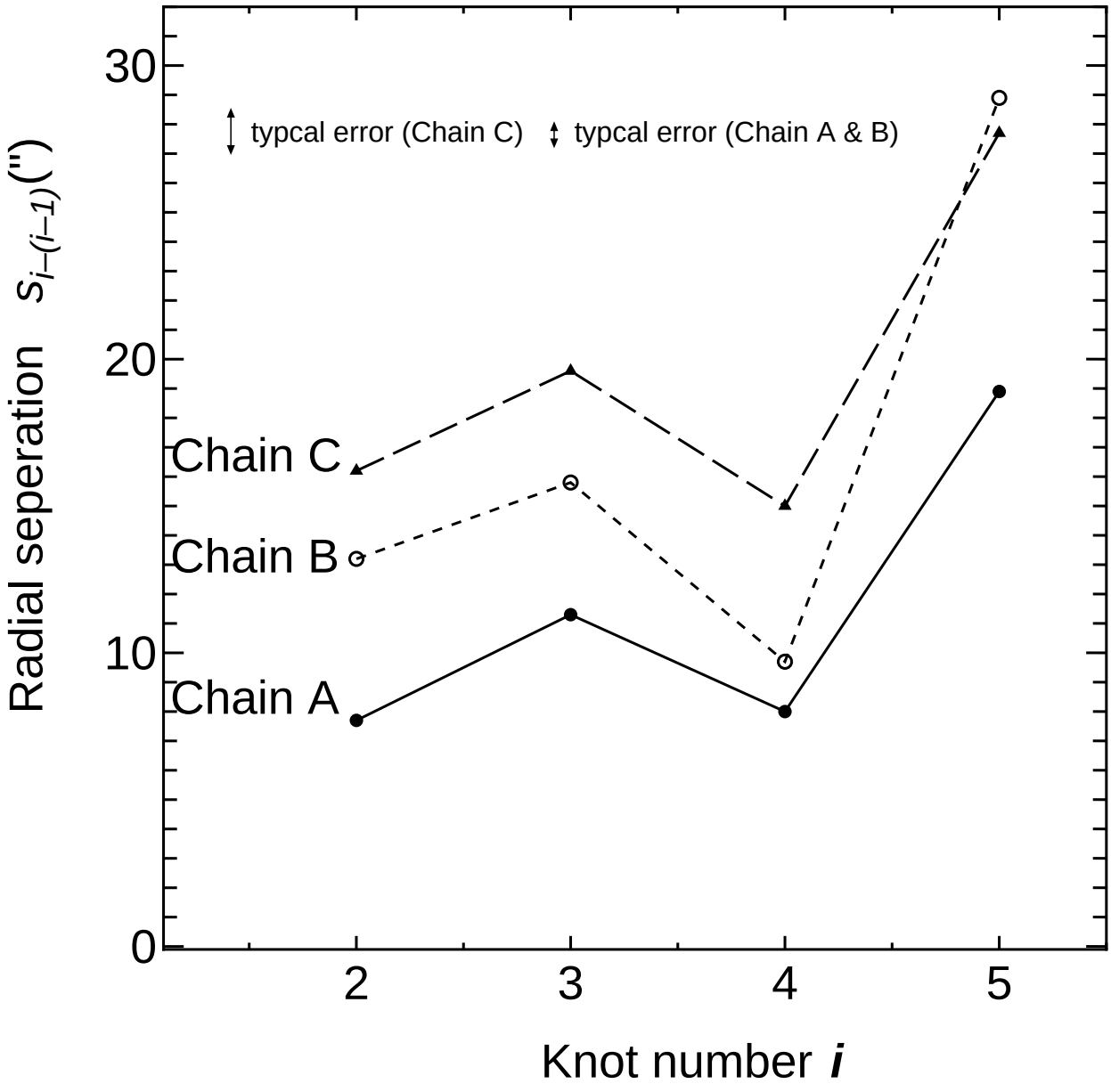
30
20
10
0
2
3
4
5
Radial seperation $s_{i-(i-1)}$(")
Knot number *i*
typcal error (Chain C)
typcal error (Chain A & B)
Chain C
Chain B
Chain A

This figure "Sudou_fig7.jpg" is available in "jpg" format from:

http://arxiv.org/ps/astro-ph/0004194v1

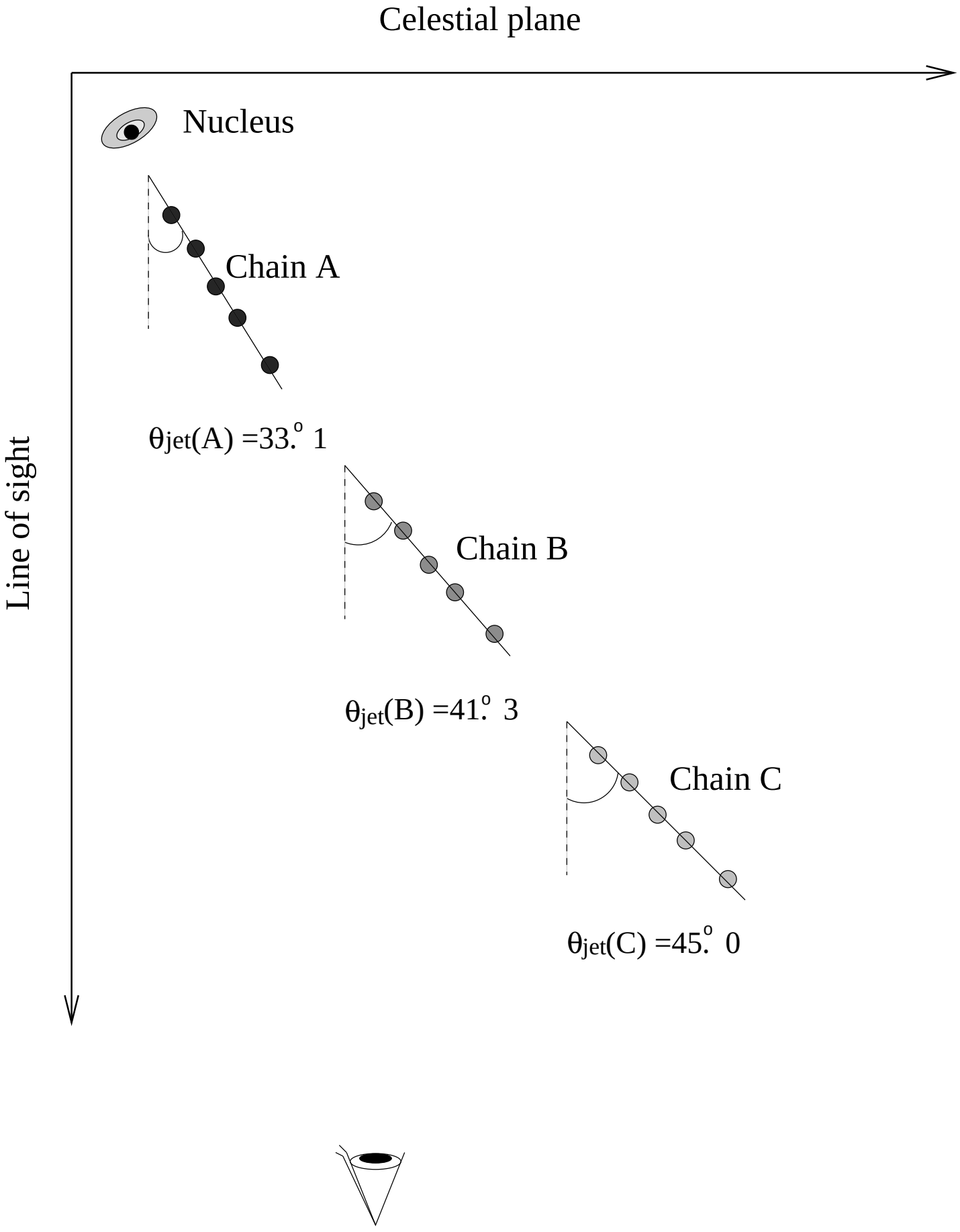
Celestial plane
Nucleus
Chain A
θjet(A) =33.° 1
Chain B
θjet(B) =41.° 3
Chain C
θjet(C) =45.° 0
Line of sight